Enhancement of the Stability of Au-Cu/AC Acetylene Hydrochlorination Bimetallic Catalyst with Melamine Treated Support

Wang, Lei•; Zhao, Jigang*+; Shen, Benxian

State Key Laboratory of Chemical Engineering, East China University of Science and Technology, Shanghai 200237, P.R. CHINA

Zhang, Yehui; Wu, Chunlei

Tianjin Dagu Chemical Co., Ltd. Tianjin, 300455, P.R. CHINA

ABSTRACT: *This paper highlights the experimental and theoretical studies on the Melamine treated Active Carbon (MAC) support for an Au-Cu bimetallic catalyst in acetylene hydrochlorination reaction. Compared to the original Active Carbon (AC) loaded with the same amount of 0.1wt% Au and 1.0wt% Cu, MAC supported catalyst (MACH), where in Carbon/$C_6H_6N_6$ mass ratio was 5:3, exhibited excellent catalytic activity. The initial conversion of acetylene increased from 77.5% to 82.7% at 150 ℃ and atmospheric pressure. The gas hourly space velocity (GHSV) was 120 h^{-1} under a feed volume ratio V_{HCl}/V_{C2H2} of 1.05. As polymerization of acetylene on the catalyst was the main cause of deactivation, accelerated deactivation test was carried out. The result indicated MACH performed good anti-coking capacity. Based on the characterization by using BET, XRD, SEM, TGA, TPD and XPS techniques, the variation of O1s XPS spectra of the synthesized catalysts was observed that was in line with DFT results. It is postulated that the better stability and the better dispersion of gold cations were ascribed to the additional metal and the modified substrate. The electron transmission from the auxiliary and the elevated groups on the catalyst surface partially inhibited the reduction of the Au^{3+} active species. Meanwhile, the stronger adsorption energy of HCl was also beneficial to catalytic activity and stability.*

KEYWORDS: *Melamine; Bimetallic catalyst; Acetylene hydrochlorination; DFT Calculation.*

INTRODUCTION

Coal-based acetylene hydrochlorination is one of the main processes to commercially prepare vinyl chloride monomer (VCM) [1], to provide the most important feedstock for polyvinyl chloride production. To meet the increasing demands for polyvinyl chloride (PVC) products, it is essential to develop more effective catalysts for this technology by using coal as a starting material. It is known that the previous industrial catalysts for this process are rapidly deactivated [2] due to the loss of volatile active components from toxic $HgCl_2$

** To whom correspondence should be addressed.*

+ E-mail: zjg@ecust.edu.cn

• Other address: Tianjin Dagu Chemical Co., Ltd. Tianjin, 300455, P.R. CHINA

1021-9986/2018/6/43-58 16/$/6.06

complexes and the resultant sublimation of mercury [3] causes severe safety and environmental concerns. In addition, the insufficient space velocity (30-50 h^{-1}) also limits the production capacity. Therefore, various new noble metal chloride catalysts, including $AuCl_3$, $PtCl_4$, $PdCl_2$, or $RuCl_3$, have been tested and developed as reported in the literature [4-9]. In the last decade, Au-based catalysts have already been studied in detail and a supported Au-based catalyst with excellent catalytic performance in acetylene hydrochlorination reaction has been applied [10-12].

However, it was observed that the reduction of Au^{3+} (as active sites) to Au^0 and the subsequent sintering resulted in a poor distribution of Au particles on the carbon support and rapid loss of activity [8]. So the loading amount of gold on the catalyst is large than 1wt% in most literature. To alleviate this problem, some other metals were incorporated into the Au catalyst to form a bimetallic Au-based catalyst [13, 14]. Gold and another metal containing bimetallic catalysts could give improved performance by their synergetic effects in the acetylene hydrochlorination reaction. The mixed metal ions were selected from Ru^{3+}, Ir^{3+}, Pd^{2+}, Pt^{4+}, Rh^{3+}, Cu^{2+} or Co^{3+} [15, 16].

It was indicated that catalyst deactivation in acetylene hydrochlorination reaction was from coke deposition due to the trouble in desorption of reactants and products as well as polymerization of the vinyl chloride. Therefore, the effect of the support on the catalyst behaviors has also been addressed in the literature. In our previous work, bimetallic catalysts with high acetylene conversion [12 15, 20] have been developed, wherein different supports, such as γ-Al_2O_3, SiO_2, and carbon under various treatments were selected [21]. In this decade, stability was reported to be further improved by using N-doped Carbon NanoTubes (CNT) as support for $AuCl_3$ [17]. And the pre-treatment of AC with urea enhanced Au/AC acetylene hydrochlorination catalyst activity and stability. Similar improvement was also observed for non-metallic catalysts [18, 19] However, the mechanisms for the introduction of N-containing species has not yet been reported.

In this work, N species and nitrogen-containing groups were introduced to the original active carbon support by post-treating with melamine to form N-doped carbon (MAC) with different ratios of $C_3N_6H_6$/AC. This product was used as the support for the Au-Cu bimetallic catalyst. This new catalyst with the loading amount of 0.1wt% Au has higher catalytic activity and better thermal stability in acetylene hydrochlorination and exhibited superior ability to inhibit the deposition of coke after the reaction. Furthermore, the related mechanisms and catalytic effect by these nitrogen-containing species have been elucidated in this work.

EXPERIMENTAL SECTION

Catalyst Preparation

Melamine-doped activated carbon was prepared as follows. A certain amount of melamine was dissolved in deionized water at a temperature of 80 °C and kept stirring until completely dissolved. Activated carbon (AC) (20-40 mesh) from coconut shell was added into the above solution mixture under vigorous stirring. Then, the obtained suspension was stirred for 15 minutes and laid in an oven for 16 hours at 120 °C. Finally, the dried AC was calcined at 600 ℃ for 1 h under a nitrogen stream in a tube furnace. Consequently, the Modified Activated Carbon (MAC) was prepared with the AC and melamine weight ratio of 5: x, where x =1, 2, 3, 4, 5. These samples were designated as 1MAC, 2MAC, 3MAC, 4MAC, 5MAC, respectively. For convenience, the 3MAC catalyst was labeled as MAC later on.

Supported Au-Cu bimetallic catalysts were prepared by using a wetness impregnation technique. Melamine-doped activated carbon (MAC) (20-40 mesh), from coconut shell was washed with dilute aqueous HCl solution to remove impurities, which were poisons for the hydrochlorination reaction [22].Bimetallic Au–Cu/MAC catalysts were prepared by impregnating with 2 mL $HAuCl_4$•$4H_2O$ (the content of Au was 49.7%) solution (1 g $HAuCl_4$•$4H_2O$/100 mL) and 20 ml $CuCl_2$•$2H_2O$ solution (6.25 g $CuCl_2$•$2H_2O$/500 ml) for 5h, and then was dried at 110 ℃, to prepare $AuCl_3$-$CuCl_2$/MAC catalyst. The different corresponding ratio was designated as 1MACH, 2MACH, 3MACH, 4MACH, 5MACH, respectively. For convenience, the 3MACH catalyst was labeled as MACH later on. For comparison, the catalyst prepared with the original carbon in the same steps as mentioned was named as ACH later on.

Catalytic tests

The catalytic performance in acetylene hydrochlorination was evaluated in a 10 ml catalyst loaded fixed-bed micro-reactor (diameter 10 mm) under the pressure of 0.1 MPa

and temperature of 150 ℃. The reactor was firstly purged with nitrogen to remove water in the reaction system. Hydrogen chloride was then passed through the reactor at a flow rate of 50 ml/min for 2 h to activate the catalyst. After the reactor was heated to 150 °C acetylene and hydrogen chloride was sent in at a flow rate of 20 and 22 mL/min respectively. The reaction product was analyzed by gas chromatography (GC-920, Al_2O_3 PLOT column). The catalyst activity was measured by the conversion of acetylene (X_{C2H2}) and selectivity of VCM (S_{VCM}) as follows:

$$X_{C2H2}=(1-\Phi_{C2H2}) \times 100\% \quad (1)$$

$$S_{VCM}=\Phi_{VCM}/(1-\Phi_{C2H2}) \times 100\% \quad (2)$$

where Φ_{C2H2} is of residual volume fraction of acetylene and Φ_{VCM} the volume fraction of chloroethylene.

Accelerated deactivation tests of the catalyst

Accelerated deactivation tests of the catalyst were performed by using the following method. Each test was carried out in a Micromeritics ASAP 2920 instrument equipped with a Thermal Conductivity Detector (TCD). A certain amount of catalyst was placed into a quartz tube and degassed in a helium flow (50 mL/min) at 250 ℃, with the temperature kept constant for 150 min. The catalyst sample was weighted after it was cooled down to 40 °C. Then, the gas mixture containing 10% C_2H_2 balanced with helium was passed over the samples at a calculated flow rate (40 mL/min) under the temperature of 300 ℃ for some certain time. Then the temperature decreased from 300 °C to 40 °C under helium stream and the coke amount deposited on the catalyst surface was measured.

Catalyst characterization

The surface area and pore size distribution were measured through nitrogen physicsorption using a Micromeritics ASAP2020 automatic system. The samples were previously degassed at 300 °C under high vacuum.

Particle strength was determined by Automatic Particle Strength Tester (ZQJ-II, Intelligent Test Factory, Dalian). Samples with a similar shape were chosen for the test. Sample kept the similar shapes and sizes of 20-40 mesh, the ambient temperature was 25 °C, the relative humidity was 70%, the loading rate for 5 mm/min.

NETZSCH TG 209 F1 Libra was used for the ThermoGravimetry (TG) study. A sample of 5-20 mg for each TG experiment was put into a platinum sample cell, which was then located on a sample pan hung inside a furnace tube under a nitrogen flow rate of 50 mL/min. The thermocouple was located next to the bottom of the platinum sample cell exposed to the nitrogen flow. Changes in the sample weight, as well as the temperature in this instrument, were continuously monitored. The temperature was ramped from room temperature to 900K with the heating rate of 10 K/min.

XRD data were collected by using a Bruker D8 advanced X-ray diffract meter with Cu-Kα irradiation at 40 kV and 40 mA in the scanning range from 10° to 80°. XPS data were collected using an Axis Ultra spectrometer with a monochromatized Al-K_α X-ray source, a minimum energy resolution of 0.48 eV (Ag $3d_{5/2}$) and a minimum XPS analysis area of 15μm. Temperature programmed analysis (including HCl-TPD)was carried out in a Micromeritics ASAP 2920 equipped with a Thermal Conductivity Detector (TCD). The sample was placed into a quartz tube and degassed in a He flows (50 mL/min) at 250 °C, with the temperature being kept constant for 15 minutes. Then, the sample was cooled down to 50 °C. The gas mixture containing pure HCl gas, flowrates of 50 mL/min was passed over the samples for 60 minutes as an adsorption gas. After being purged with pure He for 90 minutes at the same temperature, a temperature ramp from 50 to 600 °C (ramp rate, 10 °C/min) for desorption under helium flow (30 mL/min).

The morphology of the samples was characterized by Scanning Electron Microscope (SEM) (NOVA NanoSEM450, FEI Company, Holland).

DFT calculation

All of the calculations were performed using program package $DMol^3$ in Materials Studio (version 7.0) of Accelrys. The physical wave functions were expanded in terms of accurate numerical basis sets in the $DMol^3$ software. The double-numeric quality basis set with polarization functions (DNP) was used here. The Generalized Gradient Approximation (GGA) with PBE exchange was implemented in the $DMol^3$ package.

The convergence criteria for configuration optimization was set to the tolerance for SCF (self-consistent field), energy, maximum force, with a maximum displacement

Table 1: Textural properties of samples.

samples	SSA,(m^2/g)	V, (cm^3/g)	Mean pore size, (nm)
AC	1038	0.415	2.07
ACH	1010	0.380	1.88
1MAC	619	0.332	2.05
2MAC	609	0.317	2.08
3MAC	575	0.299	2.08
4MAC	545	0.265	2.05
5MAC	527	0.228	2.05
MACH	573	0.200	2.00

of 10^{-5} Ha,1.0×10^{-6} Ha and 0.002 Ha/Å, respectively.

In order to investigate which metal chloride was easier to provide electron to $AuCl_3$, the difference of energy gap (EG) was calculated as shown in Eq. (3):

$$EG = LUMO_{AuCl_3} - HOMO_{MCl} - \left(LUMO_{MCl} - HOMO_{AuCl_3}\right) \quad (3)$$

Where EG was the total energy of the base of electronic transmission from the co-metal to the active species. The more positive the EG was, and the corresponding metal chloride (MCl) was more suitable for use as an additive. The electron density on the Highest Occupied Molecular Orbital (HOMO) and Lowest Unoccupied Molecular Orbital (LUMO) responded to the pros and cons of electronic ability for metal chlorides.

The adsorption energy (E_{ads}) for atoms or molecules on was calculated as follows in Eq. (4):

$$E_{ads} = E_{HCl/MCl} - E_{HCl} - E_{MCl} \quad (4)$$

In the above equations，E_{MCl}, E_{HCl} and $E_{HCl/MCl}$ were designated as the energy of metal chlorides, the energy of HCl, and the total energies between HCl and Metal chlorides respectively.

And the bond strength values of phenolic groups and carboxylic groups were calculated using the Formula (5):

$$BS(\text{bond strength}) = E(\text{cluster}) + E(\text{adsorbate}) - E(\text{adsorbate on cluster}) \quad (5)$$

where E (cluster), E (adsorbate) and E (adsorbate on the cluster) indicate the energy of cluster, the energy of adsorbate and the total energies of adsorbate on the cluster respectively.

RESULTS AND DISCUSSIONS

Effect of melamine treated support

Table 1 listed the textural properties of AC, ACH, melamine treated the AC (MAC). It indicated that AC had a microporous structure, with a specific area (SSA) of 1038 m^2/g. After loading the active component on the AC, the specific area of ACH decreased slightly from 1038 m^2/g to 1010 m^2/g, due to the active species filling or blocking part of the pores. The specific area of 1MAC decreased sharply from 1038 m^2/g to 619 m^2/g as melamine treated AC. The specific surface areas of MAC decreased with an increase in the amount of doping melamine. This also meant that the melamine was successfully doped and in a state on the AC surface. It also should be paid attention that MACH had a large pore size of 2.00 nm compared with ACH of 1.88 nm, the decreased surface area, and increased pore size may be ascribed to part of the micropores disappear and destruction of the cell wall. The results indicated that after treatment and impregnation of the catalyst with melamine, the textural properties of carbon had been changed, especially in the surface area. Their catalytic activity should be required for further investigation.

The mechanical strength changes of the samples were tested by Strength Tester, and the effects of AC pretreated by different melamine on radical compressive strength were shown in Fig. 1. It can be seen that there was no obviously changes in the compressive strength of the sample particles. Therefore, with the increased ratio of AC/melamine, the structured supports and catalysts also showed similar mechanical strength with the original carbon, which agreed well with the fact that AC pretreatment with melamine has no obvious affect in material mechanical strength.

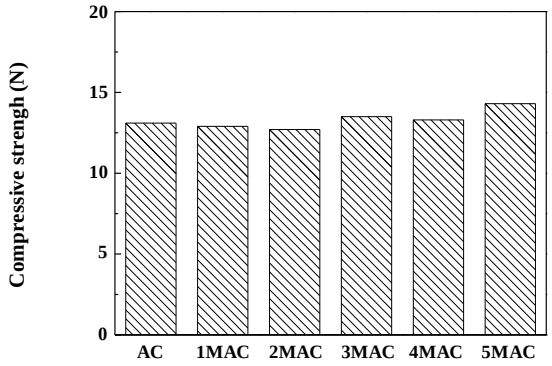

Fig. 1: Effects of AC pretreated by different melamine on radical compressive strength.

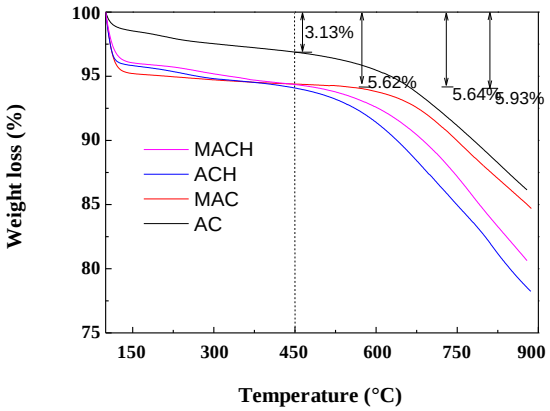

Fig. 2: TGA curves of AC, MAC, ACH and MACH samples.

Thermal analysis was also employed to obtain information on the stability of the samples. The TG profiles of both supports and catalysts are all shown in Fig. 2.

The catalyst of MACH and ACH showed a similar slight weight loss as support (MAC and AC) with two distinct curves from Fig. 2. A comparative analysis of the TGA curves presented in Fig. 2, it showed that the mass losses of AC, MAC, ACH, and MACH in the range of 100-450 ℃ were 3.13%, 5.64%, 5.93%, and 5.62%, respectively, and the remaining part of the TGA curves in the range of 600-900 ℃ of samples reflected thermal decomposition of carbon materials. For comparison, after being treated with melamine, MAC (5.64%) showed poorer thermal stability than the original carbon (3.13%). It was consistent with the destruction of the cell wall in BET results. It indicated that active ingredients decomposed which could cause the weight loss according to the ACH loss weight of 5.93% and the AC loss weight of 3.13%, while there was little difference between the loss weight of MACH (5.62%) and MAC (5.64%). Therefore, it can be referred that the thermal stability of modified supports could inhibit active ingredients loss in some way. Furthermore, we have already mentioned that MAC has no obviously affected textural properties in Fig. 1 and Table 1, so the modified support (MAC) and the structured catalysts may be the more promising for the possible industrial application resembling the application of AC.

Effect of melamine treatment on the catalytic performances

The catalytic performance of Au-Cu/MAC catalysts with different weight ratios of carbon/melamine for acetylene hydrochlorination was shown in Fig. 3a. It can be seen that acetylene conversion did not exhibit a gradually improved trend as the increasing mass ratio of $C_6H_6N_6$/AC. With a Carbon/$C_6H_6N_6$ mass ratio of 5:3, the maximum acetylene conversion of 3MACH was 82.7%. Excessive $C_6H_6N_6$ in support would give a negative effect for acetylene hydrochlorination, which was ascribed to the decreased surface area in Table 1. It indicated that carbon treated with melamine should be in a suitable ratio to perform the optimal catalytic activity. The acetylene conversion of MACH and ACH was compared in Fig. 3b. It should be mentioned that MACH kept an acetylene conversion as high as 82.7% despite its only 0.1% Au weight loading, while ACH kept an acetylene conversion of 77.5%. Additionally, it can be seen in Fig. 3c that VCM selectivity of all the samples all consistently stayed at a high level of above 99%. It should be noted that in a high GHSV of 120 h^{-1}, MACH which took the MAC as the support showed higher catalytic activity for acetylene hydrochlorination than ACH which corresponds to AC support.

Effect of melamine treatment on the catalyst for accelerating deactivation of deposition

Studies [4,14] found that C_2H_2 played an important role in the catalyst deactivation through resulting in the active Au^{3+} species reduction and the polymerization formed in the acetylene hydrochlorination reaction. Accordingly, catalyst accelerated deactivation experiment was carried out and the coke deposited on the deactivated catalysts was quantitatively analyzed between MACH and ACH, the analysis results of supports were shown in Fig. 4.

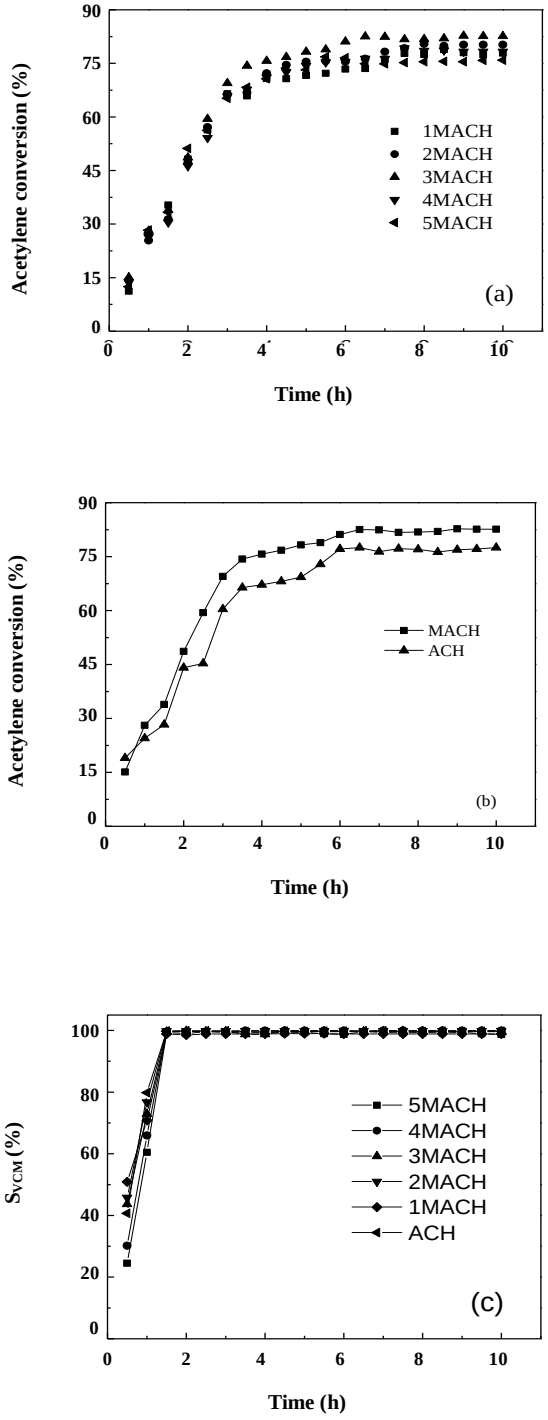

Fig. 3: Catalytic performance of catalysts: conversion of acetylene over (a) 1MACH, 2MACH, 3MACH, 4MACH, 5MACH and (b) MACH and ACH comparatively, and selectivity to VCM (c) with running time. Reaction conditions: Temperature of 150 ℃, the gas hourly space velocity of 120 h^{-1}, atmospheric pressure, feed volume ratio V_{HCl}/V_{C2H2} of 1.05.

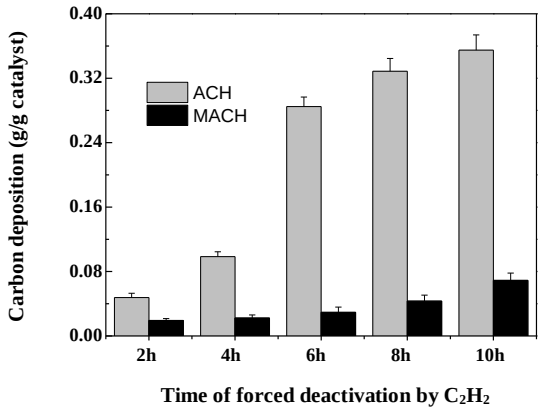

Fig. 4: The amount of coke deposition of MACH and ACH after forcing inactivation experiment.

As we can see, in a series of experiments from lasting 2 hours to 10 hours, when the catalysts were deactivated for the same reaction time, the accumulation of the coke (0.019wt% to 0.069wt%)in the used MACH was obviously reduced in contrast to the coke (0.047wt% to 0.35wt%) in the ACH, which would be especially beneficial to stabilize and prolonged the catalyst in the reaction. Hence, MACH had a better catalyst lifetime and stability, the further details would also be discussed in the subsequent section.

The morphology of the deposition on the catalysts was further investigated by SEM. The SEM micrographs of ACH and MACH catalyst with time on stream were shown in Fig. 5. SEM images of ACH catalysts with the accelerating deactivation reaction time of 2h (Fig.5a) revealed that the catalyst surface of massive amorphous, stacked and irregular features, while MACH was observed partial carbon tubes on the catalyst relatively, but only at the inlet part of the catalyst. It should be mentioned that even the accelerating deactivation reaction time of 6 hours, MACH in Fig.5c also had a comparatively smooth surface compared with ACH in Fig.5a. This result again demonstrated that the pretreated catalyst (MACH) could inhibit the formation of the deposition on the catalyst.

Catalyst Characterization

XPS

The XPS were employed to study the state of C and N ions, and the C1s (a) and N1s (b) spectra of MACH was showed in Fig.6. Meanwhile, the quantitative summary

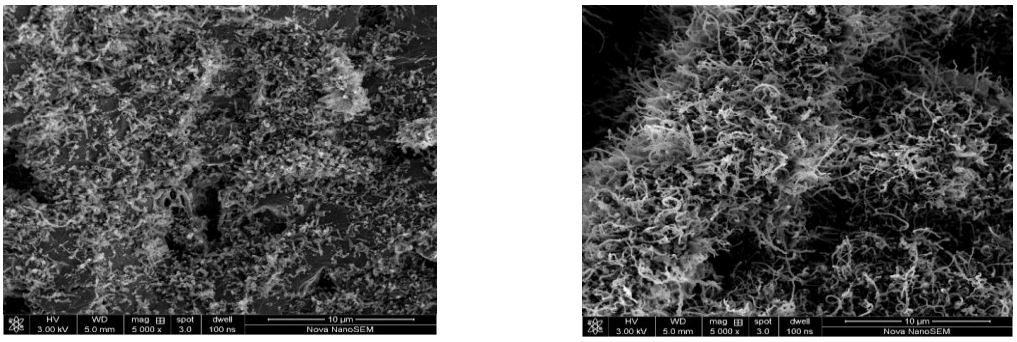

a. Used ACH 2h

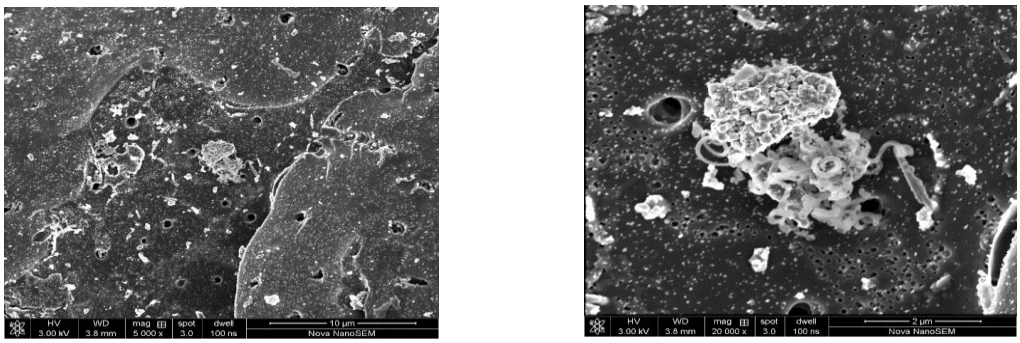

b. Used MACH 2h

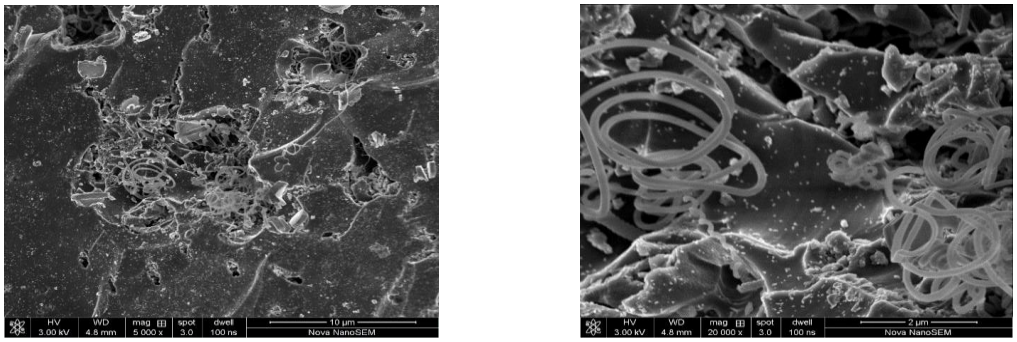

c. Used MACH6h

Fig.5: SEM images of the ACH and MACH (a) Used ACH 2h (b) Used MACH 2h.

of XPS results were listed in Table 2. It can be seen from Table 2 that the MACH catalyst surface had 7.61% N content, while no discernible N reflection detected in the original AC, this indicated that nitrogen signal can be clearly detected. As the loading amount of melamine increased, the nitrogen content of the modified supports changed from 5.04% to 8.81% then to 6.91%. And the catalytic activity in Fig. 3 also supported this characterization result. When the ratio of melamine/AC increased to a certain extent, nitrogen content was a little visible increase. Considering the additions of melamine, it was also characterized by N1s (b) and C1s (a) XPS.

Table 2: Surface C and N composition of fresh ACH and MACH catalyst, determined by XPS.

Samples	Elemental composition (wt%)	
	N1s	C1s
$C_6H_6N_6$	64.59	33.52
1MAC	5.04	83.32
3MAC	8.81	87.16
5MAC	6.91	82.29
MACH	7.61	91.87

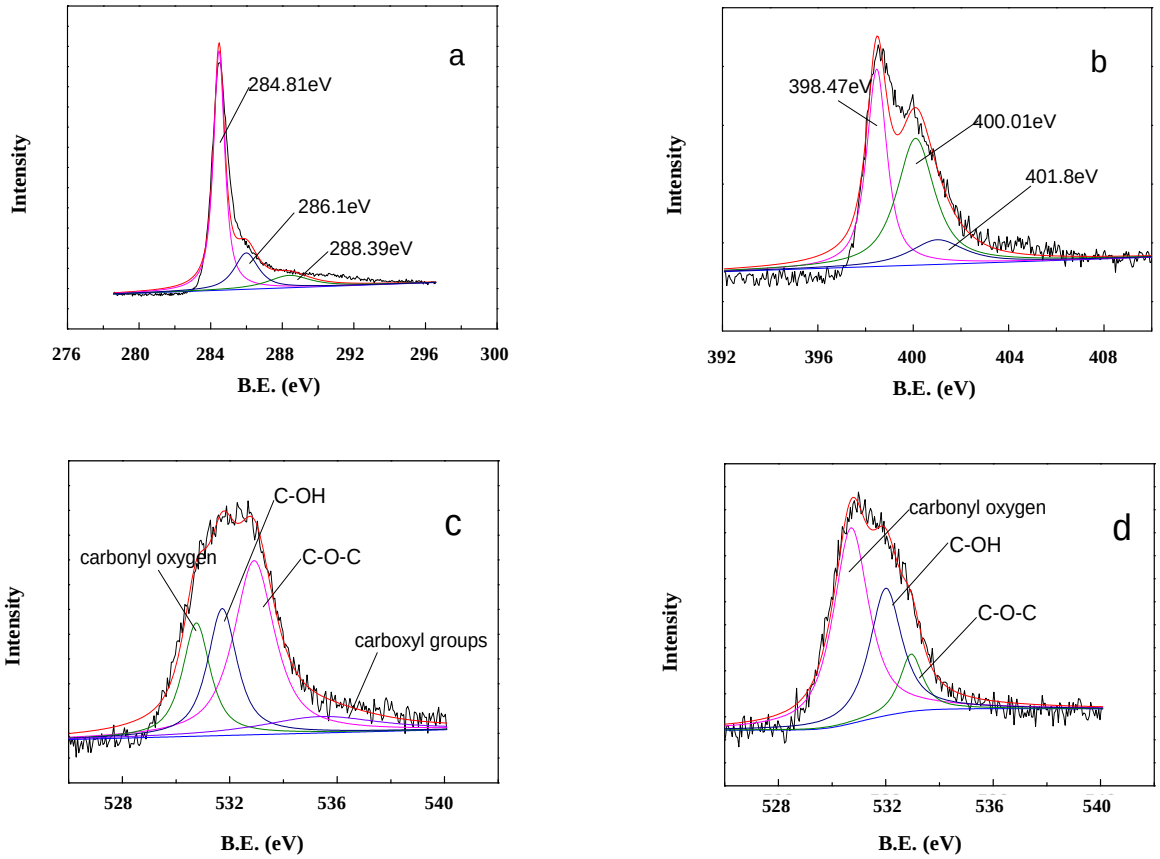

Fig.6: (a) C1 XPS spectra of MACH, (b) N1 XPS spectra MACH, (c) O1s XPS spectra of ACH, (d)MACH

The analyses on the different samples have shown the following peaks: (1) In Fig. 6a, the MACH presented three characteristic peaks at 284.80 eV, 285.99 eV and 288.39 eV, in which peaks at 284.81 eV, 286.1 eV corresponding to the original C-C (284.81 eV) and C-OH (286.1 eV) bonds, simultaneously C-N-C bond was present at 288.39 eV[12]. (2) As Fig. 6b shown, three types of nitrogen species coexist in the MACH catalyst. The spectra with binding energies at 398.47 eV, 400.01 eV, 401.8 eV were assigned to pyridinic nitrogen, pyrrolic nitrogen which bonded to three carbon atoms, and primary amine groups. (3) Taking oxygenic groups into consideration [23], O1s XPS spectra of ACH and MACH were also compared. For oxygen, the deconvolution of the O1s spectra yielded the following four peaks: the binding energy around 531.0-531.9 eV, 532.3-532.8 eV, 533.1-533.8 eV, and 534.3-535.4 eV represent carbonyl oxygen of quinines, C-OH phenol groups, C-O-C ether

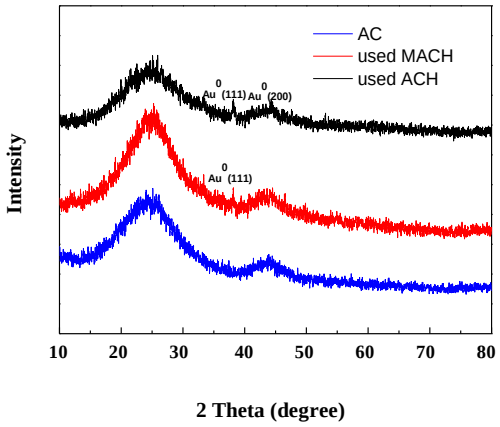

Fig. 7: XRD patterns of AC and used MACH and used ACH.

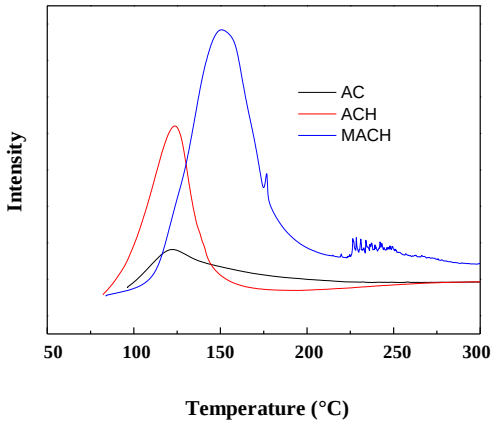

Fig. 8: TPD profiles of hydrogen chloride on different samples: ACH, AC, and MACH.

groups and carboxyl groups [24-26]. After the modification, the relative amount of carboxyl groups decreased significantly and the carbonyl oxygen of quinines, C-OH phenol groups increased. For carbonyl oxygen of quinines, the relative content increased from 19.7% to 62.9%, which may be beneficial for removing or changing carboxylic groups from the surface by melamine treatment.

MACH conducted the highest catalytic activity and previous studies showed that the activity of the Au-based catalyst was beneficial for Au^{3+} species, The activity of Au-based catalysts for acetylene hydrochlorination reaction decreases along this order: $Au^{3+} > Au^{+} > Au^{0}$.[13] Thus the XRD patterns of carbon support, the used ACH and used MACH catalysts after running 10h were displayed in Fig. 7 to investigate the status of active sites in the corresponding catalysts.

It can be seen that the X-ray patterns of support, ACH and MACH were also roughly similarly with the typical features of active carbon [17] in Fig. 7.

The ACH presented two distinct peaks at 38.12°, 44.34°[16] which are assigned to Au (111), Au (200) planes, respectively. In contrast, for MACH catalyst, the two broad diffraction peaks are marginally differentiable from the background, as shown at 38.12° The XRD result obtained in this work could also confirm that reduction exists in Au-based catalysts, and the reduction of Au^{3+} in a catalyst with melamine, treatment could be inhibited. It noted that MACH could perform a more durable activity in comparison to the freshly Au-Cu/AC.

HCl-TPD

Studies on the deactivation mechanism of $AuCl_3$ catalyst in the reaction showed that $AuCl_3$ catalyst with melamine treatment can efficiently adsorb HCl molecule, the deactivation of the $AuCl_3$ catalyst will be effectively avoided. In that case, hydrogen chloride TPD profiles for ACH, AC and MACH were presented in Fig. 8. The desorption temperature in the TPD profiles reflects the binding strength of the adsorbed species on the catalyst surface and the peak area correlates with the amount of adsorbed species. As shown in Fig. 8, areas for MACH were significantly larger than ACH and AC. Additionally, hydrogen chloride desorption temperatures increased as followed: AC <ACH < MACH, noting that MACH showed the better ability of HCl adsorption. The MACH catalyst covered the temperature range of 210-250 °C, which was higher than the temperature of 150 °C in evaluation experiment, indicating that the hydrogen chloride was strongly adsorbed in MACH and had a larger temperature range of adsorbing HCl. Therefore, MACH had an enhancement in HCl adsorption and desorption temperature after melamine treatment. Contacted with proven deactivation mechanism, it also confirmed MACH could perform more durability catalytic activity.

DFT calculation

In the acetylene hydrochlorination (As shown in Fig. 9), HCl and an $AuCl_3$ dimer co-catalyze C_2H_2 and a chlorovinyl intermediate was produced. If the HCl

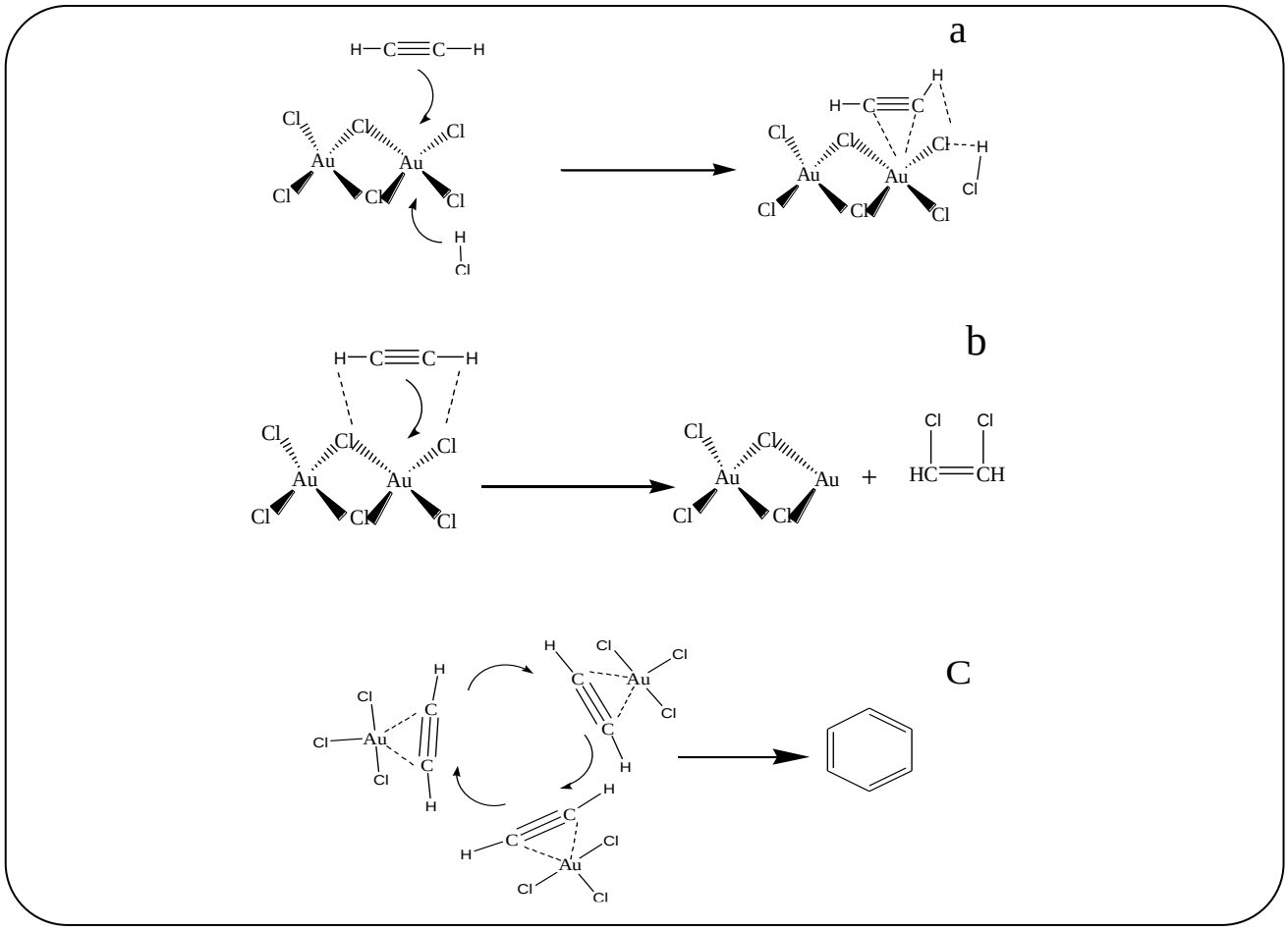

Fig. 9: Schematic of hydrochlorination of acetylene: Catalytic reaction mechanism(a), The process of Au3+ reduction(b) and The aromatization reaction (c).

in the gaseous phase could not adsorb on the Au site, chlorovinyl was difficult to desorb from the catalyst by conversion to C_2H_3Cl. The aromatization reaction would lead to coke deposits of aryne and polycyclic aromatic hydrocarbons and the reduced state of the catalyst. Thus the addition of a promoter and modifying the carbon support were two approaches to enhance the catalytic stability of the $AuCl_3$ catalyst.

Previous studies[27] have revealed that $AuCl_3$ is the electron donor in the adsorption process of hydrogen chloride. An increase of Au^{3+} electron density strengthened the bond between hydrogen chloride and $AuCl_3$. Thus, by increasing the electron density of the Au^{3+} center could inhibit Au^{3+} reduction caused by the more priority adsorption of acetylene on $AuCl_3$. The DFT was employed to obtain information about surface oxygenated groups energetics of the melamine-modified carbon, the adsorption energy of the reactants and products and electron donating ability of the co-metal and substrate in this work. Those calculations were performed to gaina further fundamental understanding of the catalytic role of co-metal and doped-N.

Select the appropriate co-catalysts for $AuCl_3$

Different metals chloride LUMO, HOMO orbital and EG levels were presented in Table 3. From the data, $CuCl_2$, AgCl, $PtCl_2$, $PdCl_4$ performed electron donating ability in contrast to other metals chloride. As a co-catalyst in acetylene hydrochlorination reaction, it was not only easier to provide electronic $AuCl_3$, but also required the greater adsorption energy of HCl to inhibit the deactivation of the $AuCl_3$ due to the loss of Cl atoms and consequently lose its activity [27]. Further, the EG associated with the adsorption ability of HCl was plotted in Fig.10.

Table 3:Different metals chloride LUMO, HOMO orbital and EG levels.

Smilation	HOMO	LUMO	$LUMO_{AuCl3}$–$HOMO_{MCl}$	$LUMO_{MCl}$–$HOMO_{AuCl3}$	EG
$CuCl_2$	-7.006	-1.428	-0.261	5.912	6.173
AgCl	-4.79	-3.722	-2.477	3.618	6.095
$PtCl_2$	-6.711	-1.308	-0.556	6.032	6.588
$HgCl_2$	-5.186	-3.293	-2.081	4.047	6.128
$LaCl_3$	-6.217	-4.757	-1.05	2.583	3.633
$PbCl_4$	-6.273	-4.654	-0.994	2.686	3.68
$PdCl_2$	-6.782	-1.167	-0.485	6.173	6.658
CuCl	-4.779	-3.818	-2.488	3.522	6.01
$BiCl_3$	-5.374	-3.215	-1.893	4.125	6.018
$AuCl_3$	-7.34	-7.267	0.073	0.073	0

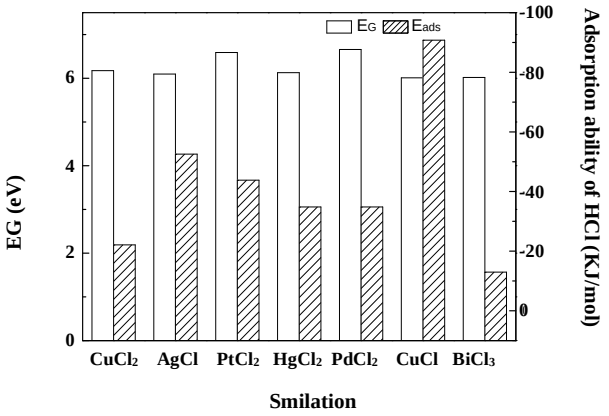

Fig. 10: Co-catalysts gold chloride for the ability of the electronic and adsorption ability of HCl.

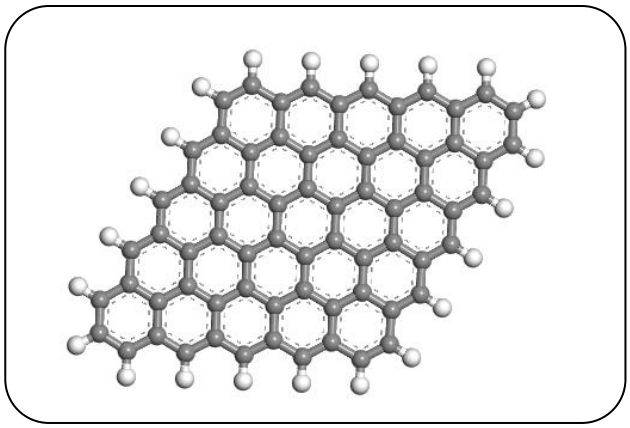

Fig. 11: Optimized structure for the graphite model (N-0), $C_{66}H_{22}$; Different bonding structures for the nitrogen: N bonded to three C atoms, two C atoms, and just one C atom, respectively.

The adsorption ability data in Fig.10 showed that although CuCl and AgCl had the weaker ability to donate electrons, they had good performance of adsorption ability to HCl. Statistically Cu, Pt, Pd should be considerable. In the meanwhile, $CuCl_2$ and $PtCl_2$ also had the catalytic ability for hydrochlorination [15,28] by itself. Based on EG and Eads, high values of both parameters should be selected as co-catalyst. Therefore, CuCl should be a promising choice. However, CuCl was susceptible to be oxidized when exposed to air. Given the above data and other factors of environment and expenses, Cu was more suitable as the co-catalyst for $AuCl_3$.

Effect of catalysts with modified carbon for acetylene hydrochlorination

Graphite models used in this work contained twenty five hexagonal rings with delocalized π electrons and terminated with C-H bonds. For modeling the nitride basal plane sheet of graphite, a nitrogen atom was placed in one of the carbon rings and different structures of various N atoms in carbon rings were displayed in Fig.11 and Fig.12 (a-d). They identified more than one bonding structures of the nitrogen: N bonded to three C atoms, two C atoms, and just one C atom, respectively. This result supported our experimental observation in XPS (Fig.6). Succinctly, four structures were named N-1, N-2, N-3, N-4.

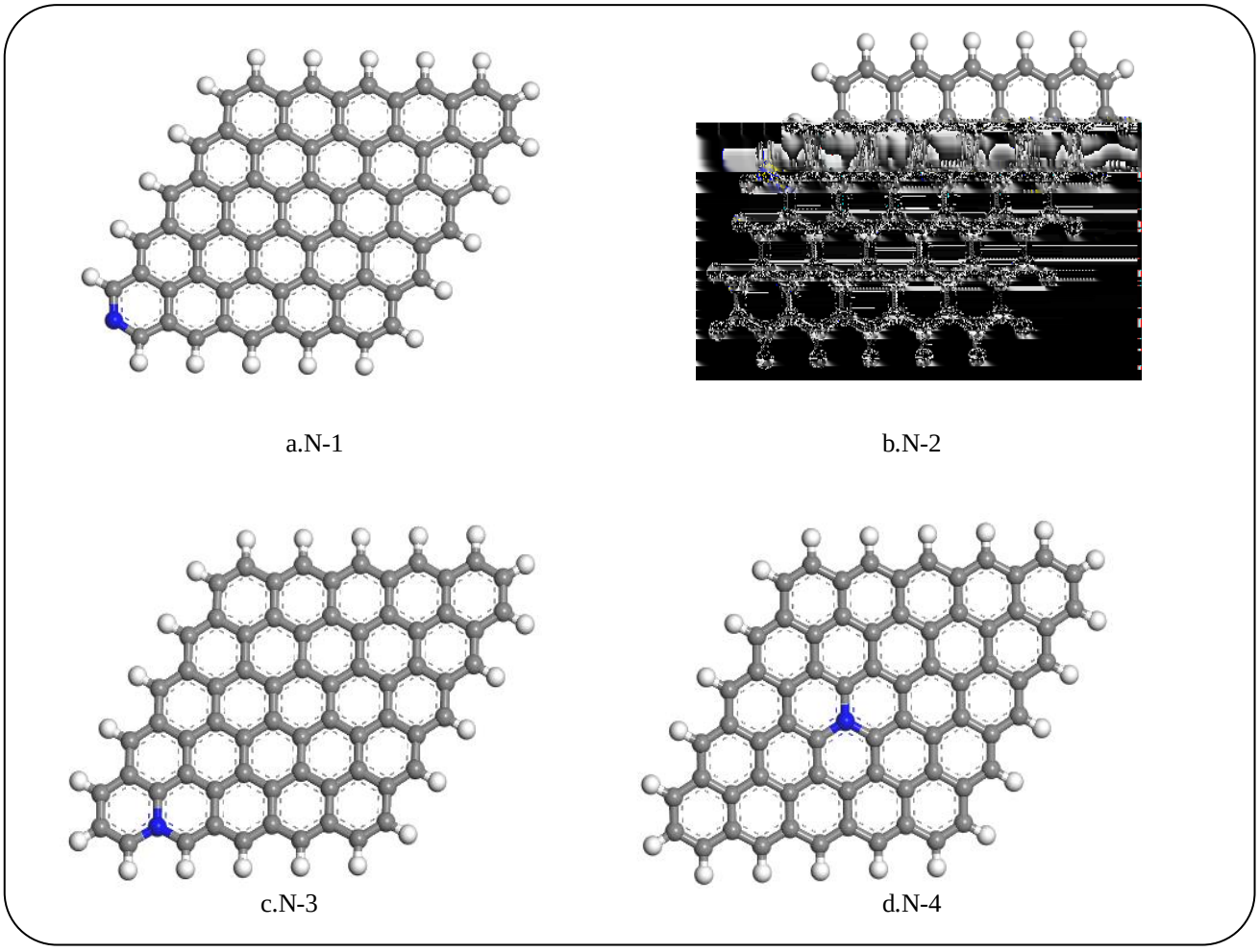

Fig. 12: Optimized structure for the N-substituted graphite model: (a) N-1; (b) N-2; (c) N-3; (d) N-4.

As expected, when graphite was doped with N, the optimized geometry was also planar and inspecting the representative structures (bond distances and changes in the structures were given in Fig.13). The bond length of C-C in N-0 was 1.430 Å, which was longer than the modified 1.417 Å in N-4. Meantime the charge appeared through C atom bonded to the N atom in N-4, three C atoms gained 0.201e, 0.201e, 0.214e, respectively. The projected density of states of this kind C atom in Fig.14 indicated that doping N induced the electronic states below the Fermi level on the carbon sites to lower energy, which meant N-4 had a better stability structure in contrast to the N-0 structure, similarly, the shorten bond length.

The adsorption energy of HCl (E_{ads}) and electron donating ability (EG) of the substrate was also discussed and the result was presented in Fig.16. For the different types, the EG decreased in the order of N-1> N-3> N-4> N-0> N-2, and no obvious enhancement in Eads for HCl occurred. The EG indicated that N-1, N-3, N-4 were more positive to compensate the charge than the fresh one among the four modified types. In contrast, the adsorption energy with E_{ads}=-460 KJ/mol and electron donating ability with EG=7.205 eV in N-0 structure and that became more facile in structure N-4 with E_{ads}= -470 KJ/mol and EG=7.609 eV owing to the more electronegative property of N atom. This suggests that from the reaction of the gas phase with the increased electron density for $AuCl_3$ and the adsorption energy towards HCl, carbon doped with N could effectively affect coke deposits and catalyze the hydrochlorination of acetylene.

Additionally, *Bulushev et al*. [23] demonstrated that phenolic groups interacted with Au^{3+} precursor by

anchoring the gold cations: ©-OH$^+$ Au^{3+}→©-O-Au^{3+}+ H^+,

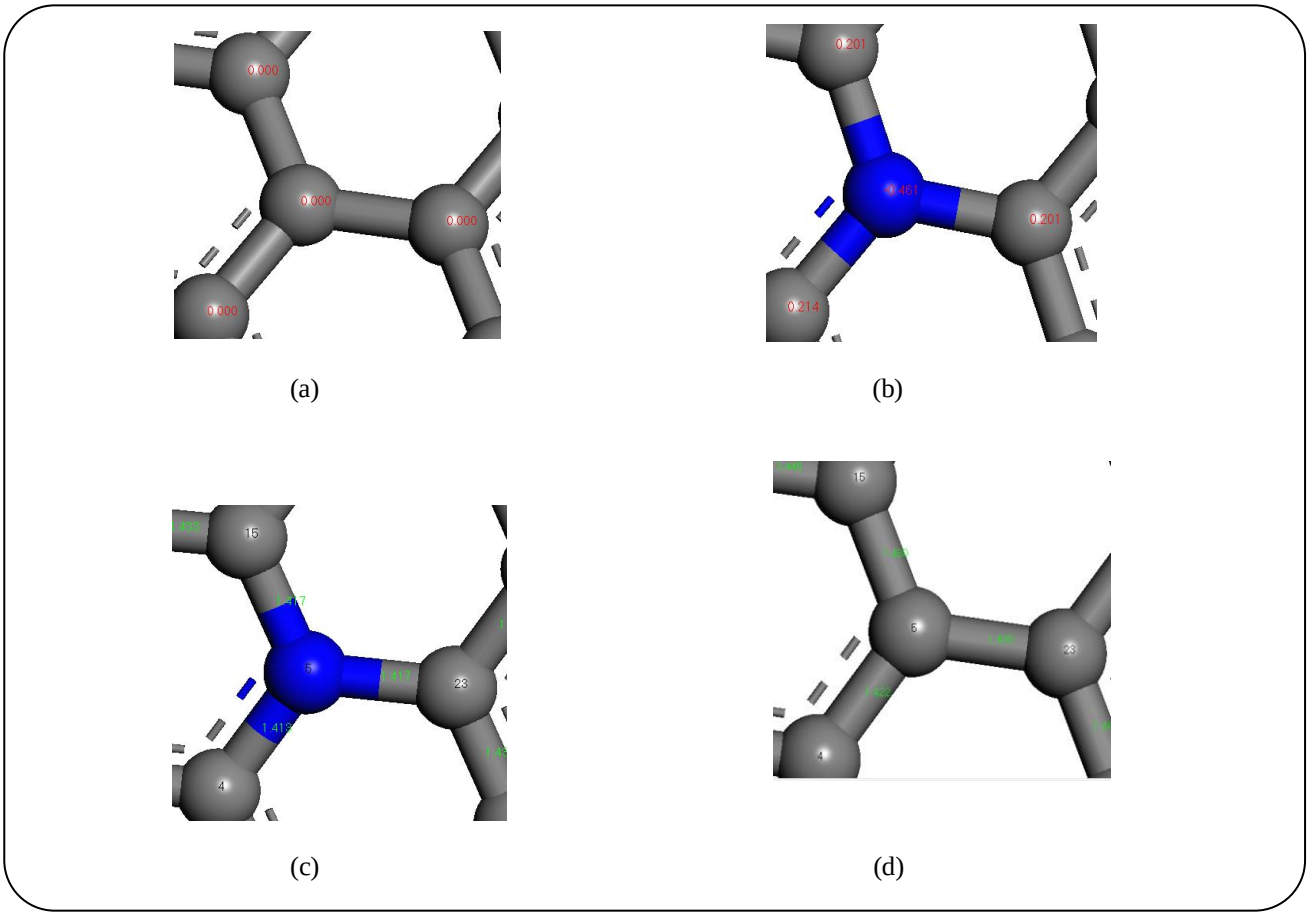

Fig. 13: Part of charge distribution of N-0 (a) and N-4 (b) and the bond distance of N-0 (c) and N-4 (d).

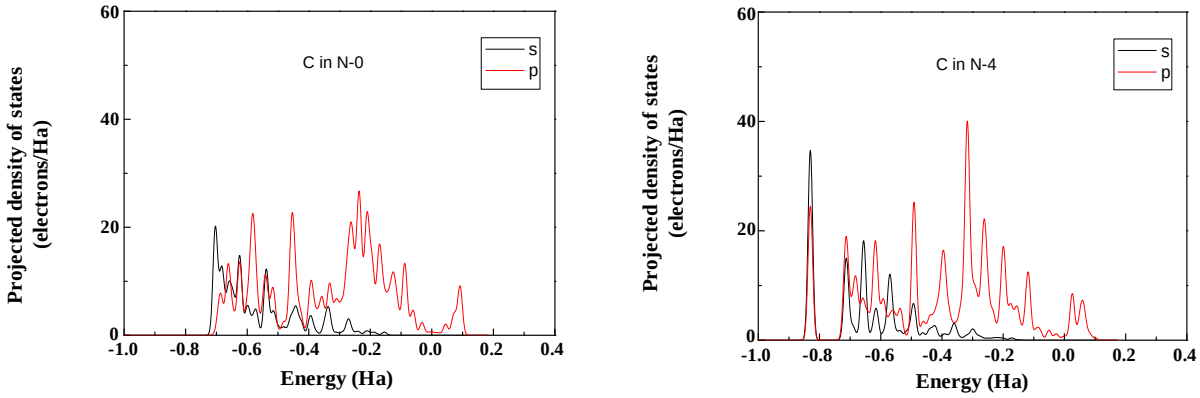

Fig. 14: The projected density of pz states of the C atom bonded to the replaced atom.

while carboxylic groups resulted in ©-COOH + Au^{3+}→© + Au^0 + H^++ CO_2↑ and also reported that phenolic groups present on the surface of activated carbon fibers were able to attach Au^{3+} to form Au-O-C [29], leading to the formation of small Au nanoparticles. From O1s XPS spectra of ACH and MACH, the difference in the amount of carboxyl and C-OH was also observed. For that case, the DFT calculation was proposed for studying the effects of surface group on a support surface with doping N treatment. The optimized structures for OH and OOH on

N-0 and N-4 surface obtained and in this study were shown in Fig.15. Because of the unsymmetric distribution

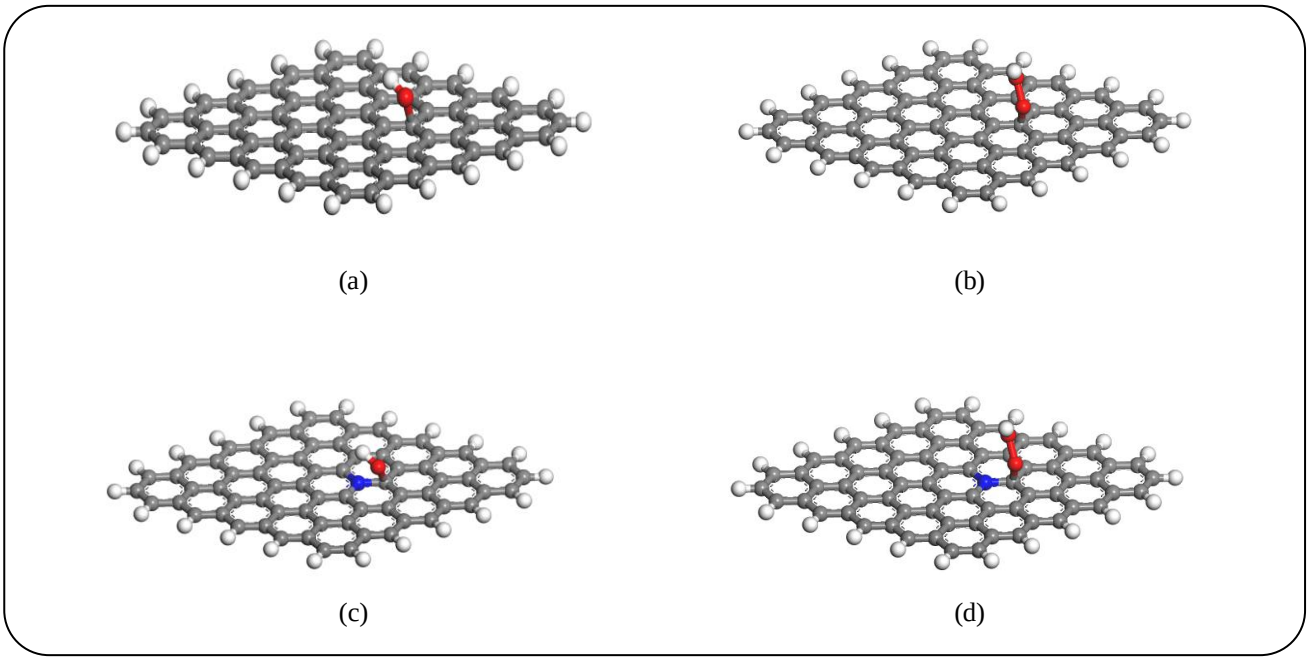

Fig 15: Optimized structure for the N-substituted graphite model: (a) OH on N-0; (b) OOH on N-0; (c) OH on N-4; (d) OOH on N-4.

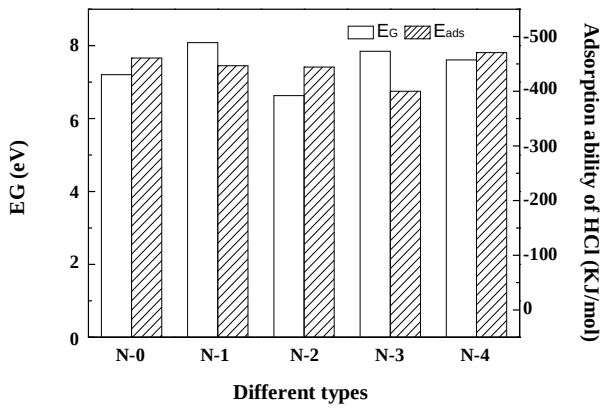

Fig. 16: Substrates for the ability of the electronic and adsorption ability of HCl.

of spin and charge densities in N-4, the distribution groups were divided into three locations: the neighbor carbon, the ortho-position, and para-position. They were noted as N-4-a, N-4-b, N-4-c and were presented in Fig.17 and the result of DFT calculations was given in Table 4. As shown in Table 4, among three C sites, OH and OOH on the carbon (N-4-a) that was directly bonded to the N atom were affected most obvious. The resulting predicted BS for OH and OOH on the undoped cluster model N-0 were 421.04 kJ/mol and 7.72 kJ/mol, while on the N-4-a were 501.73 kJ/mol and -89.16 kJ/mol. This result indicated that when doped N on the N-0 model, the bond strength for OH and OOH bond to the C atom which was adjacent to the N atom was enhanced and weakened respectively. Furthermore, according to the studies [22, 29], the better catalytic effect of doped could be attributed to the weakened BS of OOH and the strengthened BS of OH. This theory and catalytic performance were perfectly conforming to the predicted DFT calculation.

CONCLUSIONS

Au-Cu bi-metal catalytic behaviors were significantly improved by using melamine treated AC support. As given in this paper, it performed a high catalytic activity under a high space velocity. At a Carbon/$C_6H_6N_6$ mass ratio of 5:3, the maximum acetylene conversion on 3MACH was 82.7%, while that for ACH reached 77.5% under the same test conditions. Good stability was also observed, resulting from fewer deposited coke in an accelerated deactivation test. Catalyst characterization by using BET, XPS, TGA, XRD and TPD techniques revealed the distinct changes both in active sites and chemical properties of the modified support (MAC) and catalyst (MACH). These results also demonstrated the successful loading of melamine onto the AC surface.

Electron density around the $AuCl_3$, surface groups on the modified support and adsorption energy of HCl were

Table 4: BS(OH) and BS(OOH) of different types.

Types	BS(OH)/kJ/mol	BS(OOH)/kJ/mol
N-0-a	421.04	7.72
N-4-a	501.73	-89.16
N-4-b	411.63	52.00
N-4-c	403.57	45.93

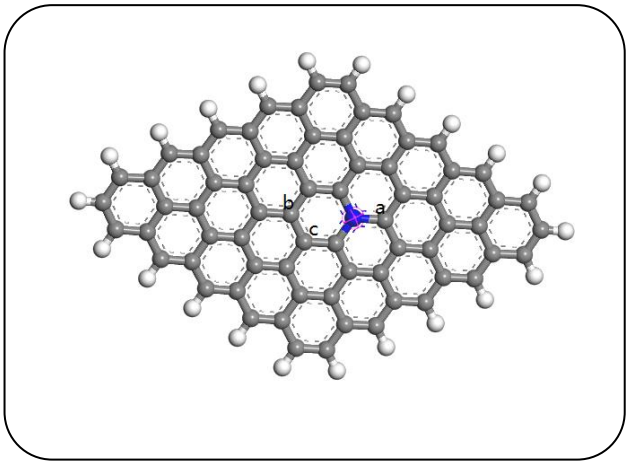

Fig 17: Three locations: the neighboring carbon (a), para-position (b), and the ortho-position (c).

the key factors in acetylene hydrochlorination reaction, the DFT calculation, based on the theories of the electronic energy gap, adsorption energy, and bond energy, elicited that $CuCl_2$ and MAC might be beneficial to the catalytic activity. Therefore, the Au-Cu/MAC catalyst could be a potential catalyst in industrial application for acetylene hydrochlorination.

Acknowledgments

The financial supported from China Scholarship Council (CSC) and Fundamental Research Funds for the Central Universities (NO. WA1214003）are gratefully acknowledged.

Received : Aug. 20, 2016 ; Accepted : Nov. 20, 2017

REFERENCES

[1] Zhang J., Liu N., Li W., Progress on Cleaner Production of Vinyl Chloride Monomers over Non-Mercury Catalysts, *Front Chem. Sci. Eng.*, **5**: 514-520 (2011).

[2] Adams M.D., The Mechanisms of Adsorption of $Hg(CN)_2$ and $HgCl_2$ on to Activated Carbon, *Hydrometallurgy.*, **26**: 201-210 (1991).

[3] Nkos, B., Coville N.J., Hutchings G.J., Vapour Phase Hydrochlorination of Acetylene with Group VIII and IB Metal Chloride Catalysts, *Appl. Catal.*, **43**: 33-39 (1988).

[4] Nkosi B., Coville N.J., Hutchings G.J., Hydrochlorination of Acetylene Using Gold Catalysts: A Study of Catalyst Deactivation, *J. Catal.*, **128**: 366-377 (1991).

[5] Conte M., Carley A.F., Hutchings G.J., Reactivation of a Carbon-Supported Gold Catalyst for the Hydrochlorination of Acetylene, *Catal. Lett.*, **124**: 165-167 (2008).

[6] Mitchenko S.A., Khomutov E.V., Shubin A.A., Mechanochemical Activation of K2PtCl6: Heterogeneous Catalyst for Gas-Phase Hydrochlorination of Acetylene, *Theor. Exp. Chem.*, **39**: 255-258 (2003).

[7] Hutchings G.J., Vapor Phase Hydrochlorination of Acetylene: Correlation of Catalytic Activity of Supported Metal Chloride Catalysts, *J. Catal.*, **96**: 292-295 (1985).

[8] Conte M., Carley A.F., Heirene C., Hydrochlorination of Acetylene Using a Supported Gold Catalyst: A Study of the Reaction Mechanism, *J. Catal.*, **250**: 231-239 (2007).

[9] Wei X., Shi H., Qian W., Gas-Phase Catalytic Hydrochlorination of Acetylene in a Two-Stage Fluidized-Bed Reactor, *Ind. Eng. Chem. Res.*, **48**: 128-133 (2009).

[10] Hutching G.J., Haruta M., A Golden Age of Catalysis: A Perspective. *Appl. Catal. A.*, **291**: 2-5 (2005).

[11] Jia J., Haraki K., Kondo J.N., Domen K., Tamaru K., Selective Hydrogenation of Acetylene over Au/Al_2O_3 Catalyst, *J. Phys. Chem.*, **104**: 11153-11156 (2000).

[12] Zhang G., Zhang J., Zhang M., Wang X., Polycondensation of Thiourea into Carbon Nitride Semiconductors as Visible Light Photocatalysts, *J. Mater. Chem.*, **22**: 8083-8091 (2012).

[13] Wang L., Shen B., Zhao J., Bi X., Trimetallic Au-Cu-K for Acetylene Hydrochlorination, *Can. J. Chem. Eng.*, **95**(6): 1069-1075 (2017).

[14] Conte M., Carley A.F., Attard G., Herzing A.A., Kiely C.J., Hutchings G.J., Hydrochlorination of Acetylene Using Supported Bimetallic Au-Based Catalysts, *J. Catal.*, **257**: 190-198 (2008).

[15] Wang S., Shen B., Song Q., Kinetics of Acetylene Hydrochlorination over Bimetallic Au–Cu/C Catalyst, *Catal. Lett.*, **134**: 102-109 (2010).

[16] Zhang H., Dai B., Wang X., Li W., Han Y., Gu J., Zhang J., Non-mercury Ctalytic Acetylene Hydrochlorination over Bimetallic Au-Co(III)/SAC Catalysts for Vinyl Chloride Monomer Production, *Green. Chem.*, **15**: 829-836 (2013).

[17] Li X., Zhu M., Dai B., $AuCl_3$ on Polypyrrole-Modified Carbon Nanotubes as Acetylene Hydrochlorination Catalysts, *Appl. Catal. B.*, **142**: 234-240 (2013).

[18] Wang X., Dai B., Wang Y., Yu F., Nitrogen-Doped Pitch-Based Spherical Active Carbon as a Nonmetal Catalyst for Acetylene Hydro -chlorination, *Chem. Cat. Chem.*, **6**: 2339-2344 (2014).

[19] Li X., Wang Y., Kang L., A Novel, Non-Metallic Graphitic Carbon Nitride Catalyst for Acetylene Hydrochlorination, *J. Catal.*, **311**: 288-294 (2014).

[20] Song Q.L., Wang S.J., Shen B.X., Palladium-Based Catalysts for the Hydrochlorination of Acetylene: Reasons for Deactivation and Its Regeneration, *Petrol. Sci. Technol.*, 28: 1825-1833 (2010).

[21] Zhao J., Cheng X., Wang L., Ren R., Zeng J., Yang H., Shen B. Free-Mercury Catalytic Acetylene Hydrochlorination Over Bimetallic Au-Bi/γ-Al_2O_3: A Low Gold Content Catalyst. *Catal. Lett.*, **144**: 2191-2197 (2014).

[22] Zhang H., Dai B., Wang X., Xu L., Zhu M., Hydrochlorination of Acetylene to Vinyl Chloride Monomer over Bimetallic Au-La/SAC Catalysts, *J. Ind. and Eng. Chem.*, **18**: 49-54 (2012).

[23] Bulushev D.A., Yuranov I., Suvorova E.I., Buffat P.A., Kiwi-Minsker L., Highly Dispersed Gold on Activated Carbon Fibers for Low-Temperature CO Oxidation, *J. Catal.*, **224**: 8-17 (2004).

[24] Lakshminarayanan P.V., Toghiani H., Pittman C.U., Nitric Acid Oxidation of Vapor Grown Carbon Nanofibers, *Carbon.*, **42**: 2433-2442 (2004).

[25] Zielke U., Hüttinger K.J., Hoffman W.P., Surface-Oxidized Carbon Fibers: I. Surface Structure and Chemistry, *Carbon.*, **34**: 983-998 (1996).

[26] Conte M., Davies C.J., Morgan D.J., Carley A.F., Johnston P., Hutchings G.J., Characterization of Au^{3+} Species in Au/C Catalysts for the Hydrochlorination Reaction of Acetylene, *Catal. Lett.*, **144**: 1-8 (2014).

[27] Zhang J., He Z., Li W., Han Y., Deactivation Mechanism of $AuCl_3$ Catalyst in Acetylene Hydrochlorination Reaction: a DFT Study, *Rsc. Adv.*, **2**: 4814-4821 (2012).

[28] Aboul-Gheit A.K., Awadallah A.E., Aboul-Gheit N.A., Solyman E.S.A., Abdel-Aaty M.A., Effect of Hydrochlorination and Hydrofluorination of Pt/H-ZSM-5 and Pt–Ir/H-ZSM-5 Catalysts for n-Hexane Hydroconversion, *Appl. Catal. A-gen.*, **334**: 304-310 (2008).

[29] Xu J., Zhao J., Xu J., Zhang T., Li X., Di X., Ni J., Wang J., Cen J. Influence of Surface Chemistry of Activated Carbon on the Activity of Gold/Activated Carbon Catalyst in Acetylene Hydrochlorination. *Ind. Eng. Chem. Res.*, **53**: 14272-1304281 (2014).